Nanotechnology, Science and Applications

Dovepress
open access to scientific and medical research

Open Access Full Text Article

SHORT REPORT

Probing wavenumbers of current-induced excitations in point-contact experiments

This article was published in the following Dove Press journal:
Nanotechnology, Science and Applications
2 June 2010
Number of times this article has been viewed

Z Wei
M Tsoi

Department of Physics, Center for Nano and Molecular Science and Technology, and Texas Materials Institute, The University of Texas at Austin, Austin, TX, USA

Abstract: We demonstrate how a mechanical point-contact technique can provide information on the wavenumber of spin waves excited by high-density electrical current in magnetic multilayers. By varying the size of point-contacts, we have been able to control the size of the excitation volume and therefore the wavelength of current-induced spin waves. This leads to a technique with *in situ* sensitivity to wavenumbers of current-induced excitations. Our detailed size-dependent measurements support the prediction that the excited wavelength is determined by the contact size.

Keywords: spin transfer torque, giant magnetoresistance, spin waves, point contact

Introduction

It is well known that the magnetic state of a ferromagnet can be affected by high-density electric current via the spin-transfer-torque (STT) effect.[1,2] For instance, current was shown to induce spin waves, precession, and reversal of magnetization in magnetic multilayered structures.[3–6] Today, a variety of resistance measurements generate a vast amount of data on such STT excitations, including experiments at high frequencies (1–60 GHz), which provide valuable information on their frequency characteristics.[7–10] Probing spatial characteristics (eg, wavenumber) of the excitations, however, represents an experimental challenge. For instance, Slonczewski[11] has argued that the current-induced wavelength is determined by the size of the excitation region where current density is high and, thus, we would require a technique capable to probe magnetization on a nanometer scale. Recently ultrafast X-ray microscopy was used to directly visualize the current-induced reversals in magnetic nanopillars with cross-sectional areas $>10^4$ nm^2.[12] Excitation regions with sizes down to ~10^3 nm^2 were probed in experiments with lithographic point-contacts.[13] Here we present an experimental technique which exploits mechanical point-contacts and allows in situ tuning of the excitation region down to 10^2 nm^2 in size.

Mechanical point-contacts were instrumental both for our original observation of current-induced excitations[3] and in providing the first data on frequencies of the current-induced spin waves.[7] In this paper, we describe how such contacts can be used to infer indirect information about the wavenumber (or wavelength) of spin waves induced by the current. By varying the size of point-contacts, we have been able to control the size of the excitation volume and therefore the wavelength of current-induced excitations. This leads to a technique with in situ sensitivity to the wavelength of excitations. Our detailed size-dependent measurements of the current-induced spin waves and analysis

Correspondence: M Tsoi
Department of Physics, The University of Texas at Austin, Austin, TX 78712, USA
Tel +1 512 232 7962
Fax +1 512 471 9637
Email tsoi@physics.utexas.edu

of the data based on three different theoretical models support the prediction[11] that the excited wavelength is determined by the size of the excitation volume.

Materials and methods

Our [cobalt (1.5 nm)/copper (2 nm)]$_{20}$ multilayered films were fabricated by radio frequency (RF) magnetron sputtering in an ultra-high-vacuum compatible system (base pressure 2×10^{-9} Torr). The films were sputtered in 5 mTorr of argon onto silicon substrates. The usual current-in-plane magnetoresistance was measured (not shown) to be about 5%. Point contacts to the multilayer film were made with a standard system[3,14,15] where a sharpened copper wire (tip) was carefully brought into contact with the film using a differential screw mechanism. The resulting contact area can be estimated from the measured contact resistance, assuming a combination of ballistic and diffusive electron transport through the contact,[14,15] as described later. For a typical contact of 10 Ω, this gives an extremely small area of about 10^2 nm^2, enabling current densities up to 10^{13} A/m^2 to be injected into the multilayer. We, and others, have observed such high densities to produce a step-increase in contact resistance corresponding to the onset of spin-wave excitations. Figure 1 shows an example of such behavior for a fixed contact size. Solid traces show variations of the contact resistance R as a function of the bias current I recorded at different applied magnetic fields B. The measurements were taken at room temperature (295°K) and in out-of-the-plane magnetic fields larger than the saturation field of the multilayer (~1.5 T). The insert to Figure 1 shows that the critical bias current $I_c(B)$, where the step-increase in R occurs, shifts linearly with B, similar to our original observations,[3] at liquid helium temperature (4.2°K).

In our present experiment, we are able to vary the point-contact size in a single experimental run. According to predictions,[1,2] the contact size defines the wavelength of the current-induced excitations and also the slope and intercept of $I_c(B)$. Thus, measuring the dependence of $I_c(B)$ on the contact size would provide indirect information on the current-driven wavelength. Next, we describe how the size of a point-contact is controlled in our experiments.

As mentioned above, a mechanical point-contact is created when a sharp metal tip is brought into contact with a multilayer sample. After establishing the initial contact (usually small) between the tip and the sample surface, the contact size can be varied (increased) by further pressing the tip to the multilayer film. The extent of the damage to the film is controlled by relative mechanical strength of the tip and the multilayer sample. By choosing a soft tip (copper)

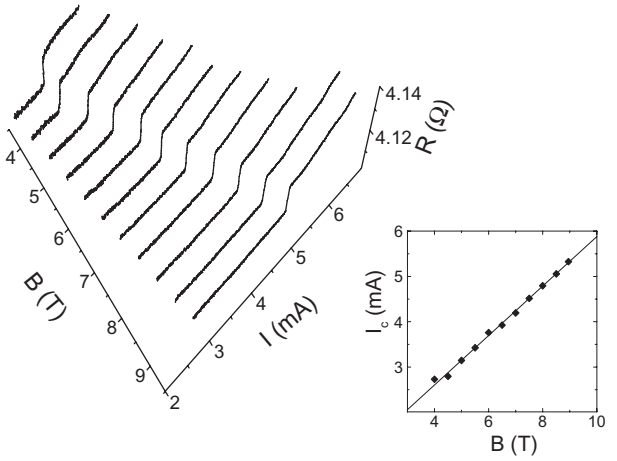

Figure 1 Current-induced excitations at different magnetic fields for a fixed contact size.

Notes: Traces show the point-contact resistance R versus bias current I at a series of applied magnetic fields B. The step increase in R corresponds to the onset of the current-induced excitations at a critical bias current $I_c(B)$. The inset shows that I_c increases linearly with B.

it is possible to minimize the damage to the sample and constrain most of deformations within the tip. The tip material is further softened by Joule heating when a high current is applied to the contact. The increase in contact size is inferred from the decrease in contact resistance, which is monitored throughout the heating procedure. This method provides a means to increase the contact size in a highly controllable manner. However, the process is irreversible, as we can only increase, not decrease, the contact size.

Using the above method to vary the size of a point-contact, we have measured $I_c(B)$ for contacts with areas ranging from 10^2–10^4 nm^2. The experimental procedure was as follows: (i) $I - V$ (current − voltage) characteristics of a contact with a given resistance $R = V/I$ are measured at different applied fields (see Figure 1). (ii) This gives $I_c(B)$ for the given R (see inset to Figure 1). (iii) The contact resistance is reduced to a new value. The measurement cycle (i–iii) is repeated to cover a wide range of resistance values. The total of seven experimental runs have shown similar results, which we discuss next for a representative contact with a wide range of resistances. Figure 2 shows $I_c(B)$ for resistance R ranging from 10.8 Ω down to 2.4 Ω. In what follows, we first describe how the contact size is defined from the measured contact resistance, then explain how the $I_c(B)$ data can be used to recover the wavelength of the current-driven excitations, and finally make a direct comparison of our results with theory.

Discussion

The problem of contact resistance, or more generally, of electron transport through the contact has been studied for

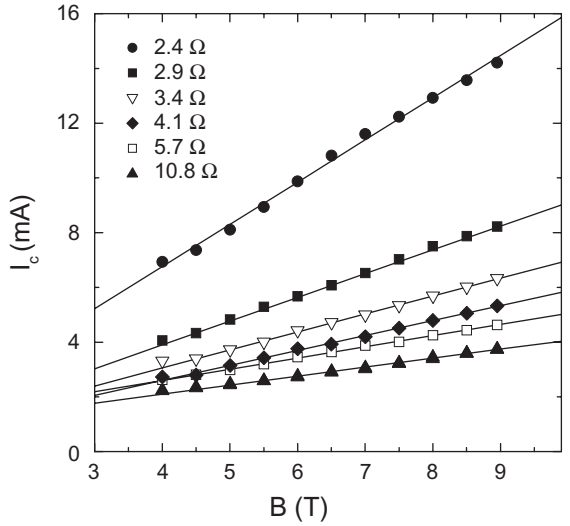

Figure 2 Dependence of critical current $I_c(B)$ for a point-contact of variable size.
Notes: Different symbols show the critical current I_c versus applied magnetic field B for a series of point-contact resistances (indicated in the legend). The contact size varies from 8 nm (for $R = 10.8\ \Omega$) to 24 nm (for $R = 2.4\ \Omega$). Solid lines are linear fits for $I_c(B)$s corresponding to different contact resistances.

more than a century. Maxwell[16] found the resistance of a circular point-contact of radius a between two large conductors when the electron mean-free-path l is much smaller than a (diffusive regime): $R_M = \rho/2a$, where ρ is the resistivity of conductors. Sharvin[17] calculated that the point-contact resistance in the ballistic regime ($l >> a$) – $R_S = 4\rho l/3\pi a^2$, where $\rho l \approx 1$ fΩ m^2, is a similar constant for most metals.[18] Nikolic and Allen[19] obtained an exact result for an arbitrary ratio l/a, that interpolates between Maxwell resistance in the diffusive and Sharvin resistance in the ballistic regime. An approximate expression for contact resistance R can be written as:[20]

$$R = \frac{4}{3\pi}\frac{\rho l}{a^2} + \Gamma(K)\frac{\rho}{2a} \qquad (1)$$

where $\Gamma(K)$ is a slowly varying function of the Knudsen number $K = l/a$, with $\Gamma(K = 0) = 1$ and $\Gamma(K = \infty) = 0.694$. Since our measurements were done at room temperature and most likely $l << a$, we use $\Gamma = 1$ in our estimations. For the contact in Figure 2, Equation 1 gives a increasing from 8 nm (for $R = 10.8\ \Omega$) to 24 nm (for $R = 2.4\ \Omega$).

By comparing the measured $I_c(B)$ dependence with the one predicted by theory, it is possible to infer the wavelength λ of the current-induced excitations. First, we obtain a slope α and intercept β of the linear fit to $I_c(B)$ data (see Figure 2). For instance, for $R = 2.4\ \Omega$, the linear fit gives $I_c = \alpha B + \beta = 15.4 \times 10^{-4}(A/T) \times B + 6.0 \times 10^{-4}(A)$. The measured values of α and β can now be compared with theory, where the slope α' and/or intercept β' of the $I_c = \alpha' B + \beta'$ dependence are expected to depend on the excitation's wavelength λ. Next, we show how three different theoretical models for the current-induced excitations can be used to elucidate λ from our data.

The first model we explore for wavelength calculations is the original spin-torque model by Slonczewski.[1,11] Here, the critical current I_c to induce spin waves in an unbounded ferromagnetic film is given as a function of applied field B and contact radius a (Eq. 13 in reference 21):

$$\boldsymbol{I}_c = \alpha'\boldsymbol{B} + \beta' = \frac{\boldsymbol{et}}{\hbar\varepsilon} 6.31\boldsymbol{a}^2\alpha_G \boldsymbol{M}_s \boldsymbol{B}_{eff} + \frac{\boldsymbol{et}_1}{\hbar\varepsilon} 23.4\boldsymbol{A} \qquad (2)$$

where $B_{eff} = B - \mu_0 M_s$, t is thickness of the excited layer, α_G damping parameter, ε spin-polarization parameter, A exchange stiffness, and M_s saturation magnetization. The model assumes that λ is equivalent to a. Using $t = 1.5 \times 10^{-9}$ m, $\alpha_G = 0.05$, $\varepsilon = 0.5$, $A = 1 \times 10^{-11}$ J/m, and $M_s = 1.45 \times 10^6$ A/m (all for cobalt), we have $\alpha' = 2.09 \times 10^{-6}\ \lambda^2$ nm^2 and $\beta' = 1.07 \times 10^{-3} - 3.8 \times 10^{-6}\ \lambda^2$ nm^2. Here both slope α' and intercept β' depend on λ and may be used to find λ from experimental data.

The second model we use for wavelength calculations explores Berger's condition for the current-induced emission of spin waves in a ferromagnetic/non-magnetic (F/N) metal multilayer.[2] Here, the energy for the spin waves comes from conduction electrons whose spin-up and spin-down Fermi surfaces are shifted (in k-space) in the direction of the current flow by a different amount due to a difference between the spin-up ($\sigma^{\uparrow}$) and spin-down ($\sigma_{\downarrow}$) conductivities in F. These shifts produce shifts of the local spin-up ($\Delta\mu_{\uparrow}$) and spin-down ($\Delta\mu_{\downarrow}$) Fermi levels at a given point of the Fermi surface. The resulting difference between $\Delta\mu_{\uparrow}$ and $\Delta\mu_{\downarrow}$ in the direction of the current flow is given by Eq. 23 in reference 2:

$$\Delta\mu = -2\left(\frac{\alpha_1 - 1}{\alpha_1 + 1}\right)\boldsymbol{j}\frac{\hbar\boldsymbol{k}_N}{\boldsymbol{en}_N} \qquad (3)$$

where $\alpha_1 = \sigma^{\uparrow}/\sigma^{\downarrow}$ is the asymmetry parameter, $\boldsymbol{j} = \boldsymbol{I}/\pi\boldsymbol{a}^2$ the current density, $\boldsymbol{k}_N$ the Fermi wave vector in N, and $\boldsymbol{n}_N$ the electron density in N.

Note that the emission of spin waves starts only when $\Delta\mu$ exceeds the spin-wave energy $\hbar\omega$. The condition $\Delta\mu + \hbar\omega = 0$ defines the critical current I_c for the excitations. Assuming a simple dispersion relation for spin waves in a thin F-film[21]

$$\hbar\omega = g\mu_B B_{eff} + D\left(\frac{2\pi}{\lambda}\right)^2 \quad (4)$$

where D is stiffness (510 meVÅ^2 for cobalt), g is Lande factor (2.170 for cobalt), and μ_B is Bohr magneton, and using $\alpha_1 = 3$, $k_N = 1.36 \times 10^{10}$ m^{-1}, $n_N = 8.5 \times 10^{28}$ m^{-3}, $D = 510$ meVÅ^2, and $g = 2.17$, we find

$$I_c = 3.0\times10^{-7} a^2 B + \frac{9.57\times10^{-4} a^2}{\lambda^2} - 10.9\times10^{-7} a^2 \quad (5)$$

Finally, our third calculation uses $\Delta\mu$ deduced from the solution of the diffusion equation for $\Delta\mu_\uparrow$ and $\Delta\mu_\downarrow$[22] as originally proposed for current-induced excitations in:[3]

$$\Delta\mu = ej\frac{2(2\alpha_F - 1)(\sigma_N^{-1}\Lambda_N)(\sigma_F^{-1}\Lambda_F)}{(\sigma_F^{-1}\Lambda_F) + 4\alpha_F(1-\alpha_F)(\sigma_N^{-1}\Lambda_N)} \quad (6)$$

where j is the current density, σ_F and σ_N are F and N conductivities, Λ_F and Λ_N are spin diffusion lengths in F and N, and α_F is the spin asymmetry coefficient in F. Assuming room temperature parameters for F = cobalt and N = copper: $\sigma_F^{-1} = 238\ n\Omega m$, $\sigma_N^{-1} = 29\ n\Omega m$, $\Lambda_F \approx 15\ nm$, $\Lambda_N \approx 350\ nm$, and $\alpha_F = 0.75$, we get $\Delta\mu = j\times3.24\times10^{-15}(eV)$ and find:

$$I_c = 1.22\times10^{-7} a^2 B + \frac{1.95\times10^{-4} a^2}{\lambda^2} - 2.22\times10^{-7} a^2 \quad (7)$$

which, along with equations 2 and 5, may be used to find λ from our experimental data in Figure 2, as we show next.

Figure 3 shows the results of our wavelength calculations. The solid line shows how the contact radius a depends on the contact resistance R according to Sharvin-Maxwell relation (Eq. 1) and will serve us as a reference. The filled symbols show the wavelength λ of current-driven spin waves calculated within Slonczewski's spin-torque model (Eq. 2) using our data from Figure 2. The filled squares were obtained from the data for the slope α' and mostly fall higher than the contact size $a(R)$ dependence. The filled triangles are from the data for the intercept β' and mostly fall below $a(R)$. The possible reason for the latter is the following: when calculating the effective field $B_{eff} = B - \mu_0 M_S$, we assumed that the F-film's magnetization M_s is fully out-of-plane. However, in reality, the magnetization is precessing and tilted away from this perpendicular-to-plane orientation that should result in a larger effective field and, thus, larger λ. For sufficiently large angles of precession, β' in Eq. 2 should be nearly independent of the contact size.

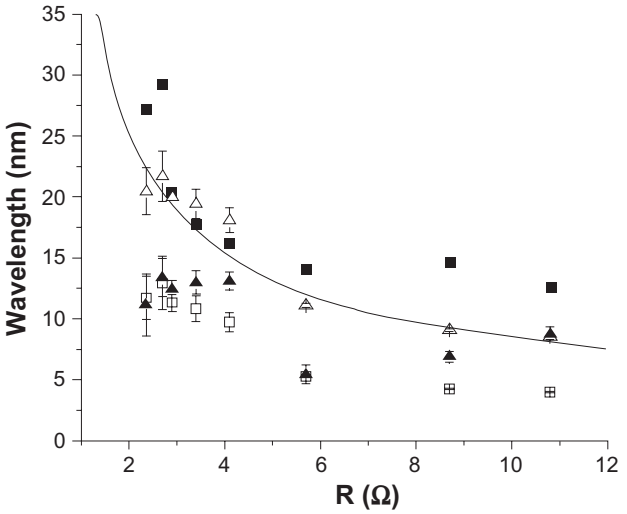

Figure 3 Wavelength λ of the current-driven spin waves versus contact (size) resistance R.
Notes: Filled squares and triangles show λ deduced from Eq. 2 and experimental data for α and β, respectively. Open triangles show λ deduced from Eq. 5. Open squares show λ deduced from Eq. 7. Solid line shows $a(R)$ from Eq. 1.

The open symbols in Figure 3 are the spin-wave wavelengths λ calculated from the $\Delta\mu = \hbar\omega$ condition. The open triangles show λ calculated within Berger's model (Eq. 5). These symbols fall the closest to the reference $a(R)$ curve. The open squares show λ obtained from Eq. 7. They all fall below the corresponding contact radius a. Since here we assumed a 100% efficiency of converting $\Delta\mu$ into the spin-wave energy, it is expected that $\lambda(R)$ will be somewhat larger for a lower efficiency realized in our room temperature experiment. Overall, the analysis of our data using all three theoretical models suggests that the wavelength λ of the current-induced spin waves is close to the size of our point-contact.

Conclusion

In conclusion, we have presented a new experimental technique which provides a means to vary the size of a mechanical point-contact *in situ* in a single experimental run. We have used the technique to perform size-dependent measurements of the current-induced excitations (spin waves) in magnetic multilayers. Analysis of our experimental data based on three different theoretical models for the excitations suggests that the wavelength of spin waves induced by an electrical current in a point-contact is determined by the contact size. This information is of importance for possible realizations of on-chip communications based on spin-wave-bus technology.

Acknowledgments

The work was supported in part by NSF Grant No. DMR-06-45377.

Disclosures

The authors report no conflicts of interest in this work.

References

1. Slonczewski JC. Current-driven excitation of magnetic multilayers. *J Magn Magn Mater*. 1996;159(1):1–7.
2. Berger L. Emission of spin waves by a magnetic multilayer traversed by a current. *Phys Rev B*. 1996;54(13):9353–9358.
3. Tsoi M, Jansen AGM, Bass J, et al. Excitation of a magnetic multilayer by an electric current. *Phys Rev Lett*. 1998;80(19):4281–4284.
4. Myers EB, Ralph DC, Katine JA, Louie RN, Buhrman RA. Current-induced switching of domains in magnetic multilayer devices. *Science*. 1999;285(5429):867–870.
5. Sun JZ. Spin angular momentum transfer in current-perpendicular nanomagnetic junctions. *J Magn Magn Mater*. 1999;202(1):157–164.
6. Wegrowe JE, Kelly D, Jaccard Y, Guittienne P, Ansermet JP. Current-induced magnetization reversal in magnetic nanowires. *Europhys Lett.* 1999;45(5):626–632.
7. Tsoi M, Jansen AGM, Bass J, Chiang WC, Tsoi V, Wyder O. Generation and detection of phase-coherent current-driven magnons in magnetic multilayers. *Nature*. 2000;406:46–48.
8. Kiselev SI, Sankey JC, Krivorotov IN, et al. Microwave oscillations of a nanomagnet driven by a spin-polarized current. *Nature*. 2003; 425:380–383.
9. Rippard WH, Pufall MR, Kaka S, Russek SE, Silva TJ. Direct-Current Induced Dynamics in Co90Fe10/Ni80Fe20 Point Contacts. *Phys Rev Lett*. 2004;92:027201.
10. Krivorotov IN, Emley NC, Sankey JC, Kiselev SI, Ralph DC, Buhrman RA. Time-domain measurements of nanomagnet dynamics driven by spin-transfer torques. *Science*. 2005;307(5707):228–231.
11. Slonczewski JC. Excitation of spin waves by an electric current. *J Magn Magn Mater*. 1999;195:L261–L268.
12. Acremann Y, Strachan JP, Chembrolu V, et al. Time-resolved imaging of spin transfer switching: beyond the macrospin concept. *Phys Rev Lett*. 2006;96:217202.
13. Mancoff FB, Rizzo ND, Engel BN, Tehrani S. Area dependence of high-frequency spin-transfer resonance in giant magnetoresistance contacts up to 300 nm diameter. *Appl Phys Lett*. 2006;88(11):112507–112513.
14. Jansen AGM, van Gelder AP, Wyder P. Point-contact spectroscopy in metals. *J Phys C*. 1980;13(33):6073.
15. Tsoi M, Jansen AGM, Bass J. Search for point-contact giant magnetoresistance in Co–Cu multilayers. *J Appl Phys*. 1997;81:5530–5532.
16. Maxwell JC. *A Treatise On Electricity and Magnetism*. Oxford, UK: Clarendon Press, 1873.
17. Sharvin YV. A possible method for studying Fermi durfaces. *Sov Phys JETP*. 21:655.
18. Bass J. *Landolt Börnstein New Series*, *Vol. III/15a*. Hellwege KH, Olsen JL, editors. Berlin, Germany: Springer; 1982.
19. Nikolic B, Allen PB. Electron transport through a circular constriction. *Phys Rev B*. 1999;60:3963–3969.
20. Wexler G. The size effect and the non-local Boltzmann transport equation in orifice and disk geometry. *Proc Phys Soc*. 1966;89:927.
21. Ashcroft NW, Mermin ND. *Solid State Physics.* New York, NY: Holt, Rinehart, and Winston; 1976.
22. van Son PC, van Kempen H, Wyder P. Boundary resistance of the ferromagnetic-nonferromagnetic metal interface. *Phys Rev Lett*. 1987;58:2271–2273.